Available online at www.sciencedirect.com

SciVerse ScienceDirect

Journal of the European Ceramic Society 32 (2012) 419–424

www.elsevier.com/locate/jeurceramsoc

Microstructure of selectively heated (hot spot) region in Fe_3O_4 powder compacts by microwave irradiation

Noboru Yoshikawa [a,*], Guoqiang Xie [b], Ziping Cao [c], Dmitri V. Louzguine [d]

[a] *Graduate School of Environmental Studies, Tohoku University, 6-6-02, Aza-Aoba, Aramaki, Aoba-ku, Sendai 980-8579, Japan*
[b] *Institute for Materials Research, Tohoku University, 2-1-1, Katahira, Aoba-ku, Sendai 980-8577, Japan*
[c] *Postdoctor at Tohoku University, Present at Graduate School of Engineering, Tohoku University, Aza-Aoba, Aramaki, Aoba-ku, Sendai 980-8579, Japan*
[d] *WPI Advanced Institute for Materials Research, Tohoku University, 2-1-1, Katahira, Aoba-Ku, Sendai 980-8577, Japan*

Received 6 March 2011; received in revised form 8 August 2011; accepted 12 August 2011
Available online 17 September 2011

Abstract

An Fe_3O_4 powder compact was irradiated with a 2.45 GHz microwave single-mode applicator at the magnetic field maximum position. Selectively heated regions (hot spot region) having several hundred micrometers to millimeter scale were formed. They exhibited metallic color. The SEM/EDX observations showed no appreciable difference in the compositions between the hot spot regions and the matrix. However, micro-XRD revealed that the hot spot region had a larger fraction of FeO than the matrix did, although the major consisting phase was Fe_3O_4 with a little Fe_2O_3. TEM observations indicated that the observed hot spot regions comprise these oxide phases separated in nano-sized grains, which agrees with our previous report. The larger fraction of FeO phase and flat surface might be related with the metallic color of the hot spot region. Their formation mechanisms and phase constitution were discussed.

Keywords: Microwave; Magnetite; Hot spot; Selective heating; Microstructure

1. Introduction

Microwave heating has been examined as a novel method for processing of various materials to provide specific functional properties because some special effects caused by interaction between the electromagnetic wave and the materials are expected to produce different microstructures and nanostructures.

Numerous reports describe the special effects observed in microwave processing of solid materials, such as enhanced rates of solid state reaction[1] and sintering kinetics.[2,3] The original mechanisms of these phenomena have been discussed.

One characteristic effect of microwave heating is so-called selective heating. Not only special phase or components of materials but also specific areas in the same substance are known to be heated selectively. This phenomenon occurs because of variation in the material properties resulting from the temperature increase. It has been discussed in relation with thermal runaway or hot spot formation. This feature is not preferred for industrial material processing because of its lack of controllability in heating and its resultant inhomogeneous products.[4]

However, from another perspective, the selectively heated area experiences rapid heating that is unattainable using ordinary heating methods. Taking advantage of this rapid heating feature presents opportunities for formation of non-equilibrium phases. For example, a supersaturated solid solution of ceramic phases is reported by microwave rapid heating.[5] Therefore, it is important to investigate the microstructures of the heated (hot-spot) regions that occur in this way because detailed discussion of the formation conditions and the detailed micro/nano-structure observation has been lacking in previous reports.

Fe_3O_4 is an objective material for microwave heating because it is a microwave-absorbing material and because it is well heated. Moreover, we are interested in microwave heating of Fe_3O_4, considering the following reports. Reportedly,

* Corresponding author. Tel.: +81 795 7343; fax: +81 22 795 7302.
E-mail address: yoshin@material.tohoku.ac.jp (N. Yoshikawa).

0955-2219/$ – see front matter © 2011 Elsevier Ltd. All rights reserved.
doi:10.1016/j.jeurceramsoc.2011.08.028

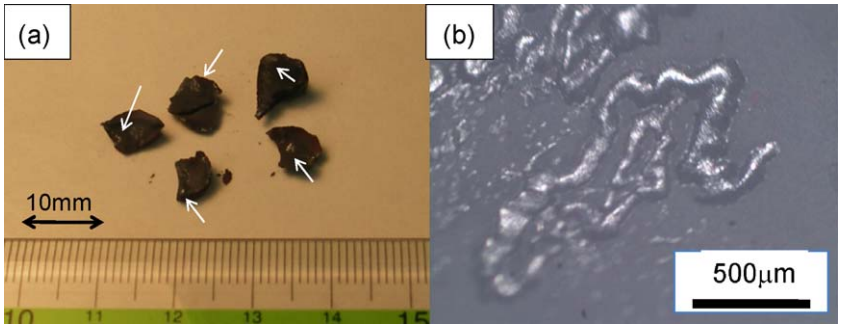

Fig. 1. (a) Photograph of microwave heated Fe_3O_4 and (b) an optical micrograph of the hot spot region ($T = 1100\,^{\circ}C$, for 1 min).

Fe_3O_4 can be reduced by microwave heating in a neutral atmosphere or in air (without reduction elements).[6] Furthermore, recently, de-crystallization phenomena[7–9] are reported which might be examples of non-equilibrium phases. Presumably, these phenomena are related to rapid heating brought about by microwave irradiation. Recently, the authors performed micro/nano structural observation of rapidly microwave-heated Fe_3O_4,[10] for which the nanoscale amorphous region and simultaneous formation of FeO and Fe_3O_4 with excess oxygen were observed.

This study was undertaken to investigate the microstructures of the rapidly heated Fe_3O_4 powder compact in a 2.45 GHz microwave *H*-field, especially devoting attention to the composition distribution and the local phase constitution in hot-spot regions. Furthermore, their constituent phases must be discussed in relation to our earlier reports.

2. Experimental

2.1. Specimens

Fe_3O_4 powder having four nines of purity (Sigma–Aldrich Japan K.K., Tokyo, Japan) was prepared, with particle size of several micrometers. The powder was loosely hand-pressed and formed into a compact rod of 5 mm diameter and 10 mm length. The compact was placed in a container cell made of SiO_2. Then the cell was thermally insulated with adiabatic material (Kaowool blanket; Isolite Insulating Products, Co. Ltd. Tokyo, Japan), which was heated once above 500 °C to remove organics, thereby avoiding carbon contamination.

2.2. Microwave heating apparatus and method

The microwave heating apparatus used for this study is a single-mode applicator with a TE10 wave guide (MKN-152-359, 1.5 kW at maximum; Nihon Koshusha Co. Ltd., Yokohama, Japan), operated at 2.45 GHz. The temperature is controlled manually with an adjusting three stub tuner, monitoring P_f, P_r, respectively denoting the forward, and the backward power. All data were recorded digitally.

Temperature measurements were conducted using an optical method (PhotoriX system; Luxtron Corp., Santa Clara, CA, USA). In this system, measurement above 350 °C is not possible. The sapphire light guide (ϕ1 mm diameter) is placed close to the specimen (ca. 5 mm) and receives light emitted from it. The light guide is separated from the specimen by about 5 mm. Fe_3O_4 specimens were heated in N_2 gas flowing conditions, and at the *H*-field maximum position in the cavity. Details are described elsewhere.[11]

2.3. Microstructural observations

The heated specimens were observed using an optical microscope (OM, BX60; Olympus Optical Co. Ltd., Tokyo, Japan). X-ray diffraction (XRD, RINT2000, CuKα radiation; Rigaku Corp., Tokyo, Japan) and XRD microdiffraction (D8 Discover, CoKα radiation; Bruker AXS, Madison, WI, USA) of the heated specimens were conducted. In the latter case, the profiles were obtained from an area of 300 μm square of the hot spot regions. Determination of the composition in local areas was conducted using EM/EDX (JSM-6500F; JEOL Ltd. Akishina, Japan).

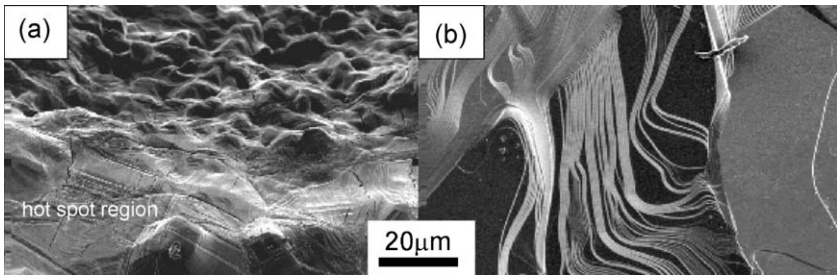

Fig. 2. SEM photographs of (a) the boundary region between the hot spot region and the matrix and (b) some morphology observed in the hot spot region.

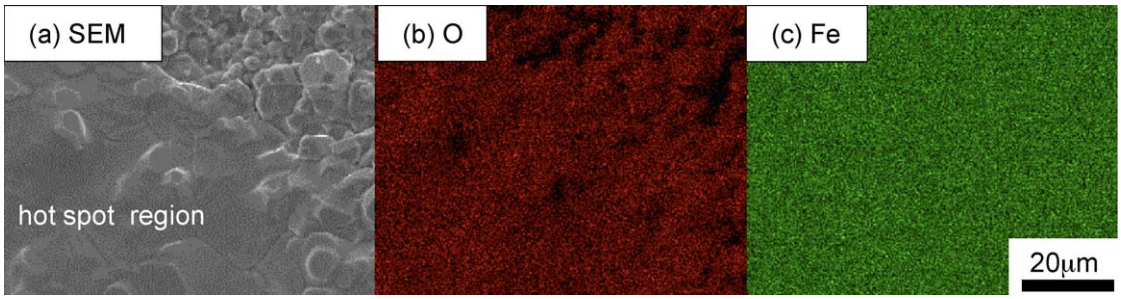

Fig. 3. SEM/EDX analysis of the boundary region between the hot spot region and the matrix. (a) SEM image, (b) EDX mapping of oxygen (O), and (c) EDX mapping of iron (Fe).

Nanometer-scale and micrometer-scale observations were made using TEM (JEM, 2010; JEOL Ltd.).

3. Results

3.1. Formation of hot spot regions having metallic color

Some regions, which have metallic color, ranging from several hundred micrometer to millimeter scale, were formed in specimens heated in the microwave *H*-field maximum position at 1100 °C for 1 min. They existed in the internal areas of the specimens (they were found in the fractured surface) in most cases. They are shown as the white regions indicated with arrows in the photograph (Fig. 1(a)). The OM photograph of the hot spot region is presented in Fig. 1(b). It must be noted that the measured temperature is the average value of sapphire rod's receiving light within its cross section, which can contain light emitted from the hot spot regions because it is possible that the hot spot region temperature is higher than the measured value.

The region was also observed with SEM. The photograph in Fig. 2(a) shows the boundary area between the hot spot region and the matrix, where a difference in flatness is readily apparent, because the matrix (upper) consists of grains having size of several micrometers or more. SEM micrographs taken from the hot spot region reveal unique features (Fig. 2(b)). Some areas have trace lines of fine steps, appearing as if certain crystalline facets had formed. They are similar to the reported morphologies of *de-crystallized* Fe_3O_4.[9]

3.2. Evaluation of microstructures

For the specimen areas that included hot spot regions, SEM/EDX analysis was performed to examine their compositional distribution. Fig. 3(a) shows the SEM image and the mapping images of (b) oxygen and (c) iron. No distinct difference of the composition (Fe/O) is apparent within the analytical limit between the hot spot region (left in the photo (a), as indicated) and the matrix (small grain) regions, which indicates that the composition is almost homogeneous over the boundary of the two regions. The oxygen in the upper right area (Fig. 3(b)) appears to be deficient. However, this results from the roughness of the grain convexity and resultant shadowing of the beam.

Phase identification using normal XRD technique was performed, the profile was obtained from the matrix and the exposed area having several millimeters' scale. An example of the profiles is presented in Fig. 4. Results demonstrated that the included phases are mostly Fe_3O_4, with some FeO. Next, the XRD microdiffraction profile is obtained from the hot spot region, an example of which is presented in Fig. 5, together with a photograph. Results demonstrated that the peak height of FeO (2 0 0) is much higher than the profile portrayed in Fig. 4 (with respect to Fe_3O_4 (4 0 0)), indicating that the hot spot region contains more FeO phase than the matrix. However, the major consisting phase is still Fe_3O_4. Some Fe_2O_3 phase also exists in the profile. The lattice constant of the Fe_3O_4 mostly accords with that of the stoichiometry. TEM observation from these areas was made. The micrograph and the diffraction pattern are depicted in Fig. 6 together with the diffraction pattern. Results show that the region consisted of nano-sized grains, and that the existence of Fe_3O_4, FeO, and Fe_2O_3 phases was confirmed by indexing the diffraction rings (which are broad and which are shown to contain these phases).

4. Discussion

4.1. Hot spot formation

According to the microstructural observation that was performed, it is regarded as appropriate to assume that a higher temperature region was formed in the specimen during microwave heating. The formation mechanism of the hot spot region is an important issue for discussion. Although its detailed mechanisms cannot be identified because of the impossibility of

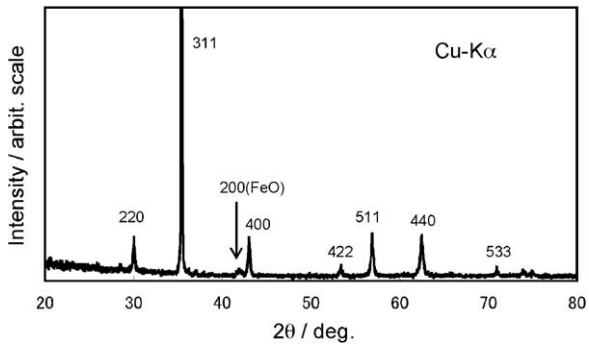

Fig. 4. XRD profile from the specimen cross section. The peaks were indexed with respect to Fe_3O_4 except the main FeO (2 0 0) peak.

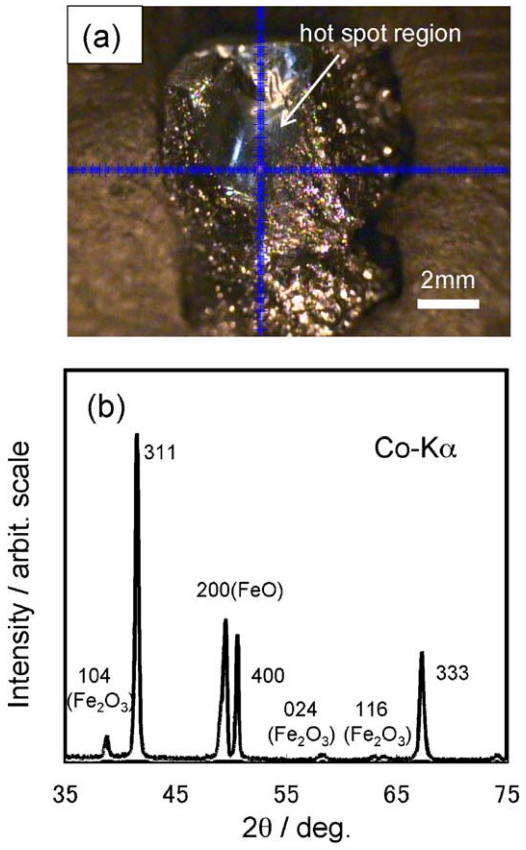

Fig. 5. Microdiffraction (XRD) analysis of the hot spot region (Co–Ka). (a) A photograph of the specimen, and (b) XRD profile from the position indicated with the crossed ruler in (a).

their in situ observation, because it occurred in the internal area of the specimen in most cases, it is inferred that the initial spatial fluctuation of the temperature giving rise to variation in the physical properties such as permittivity (ε), magnetic permeability (μ), and electric conductivity (σ) caused the variation in microwave absorbability and that the occurrence of locally accelerated heating caused the hot spot. The fluctuation can originate from some factors such as the local density difference of the powder particles in the compacts.

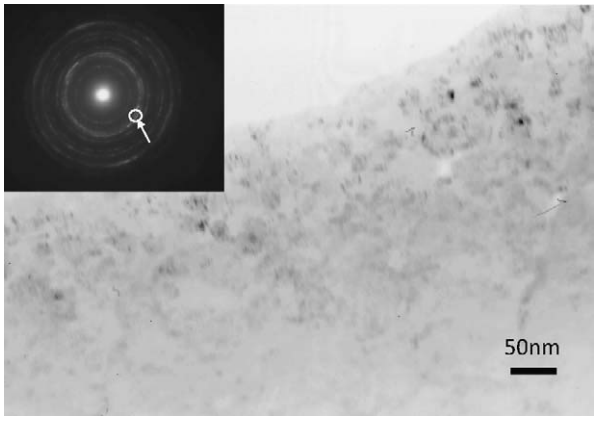

Fig. 6. TEM photograph from the hot spot area which reveals nano-gains and electron diffraction (ED) pattern, thick ring in ED pattern indicated with an arrow contains the rings from Fe_3O_4 (3 1 1), FeO (1 1 1) and Fe_2O_3 (1 1 0).

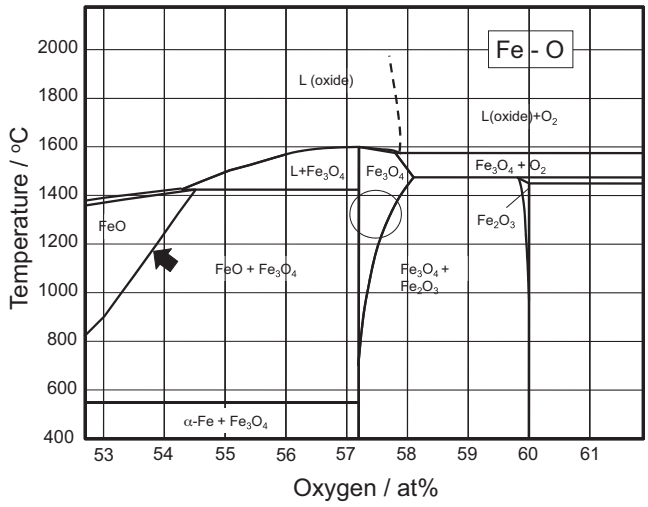

Fig. 7. Fe–O phase diagram.[13]

Generally, microwave heating mechanisms (P: power absorbed in a unit volume) are expressed in terms of the following equation[12] as

$$P = \pi\varepsilon''\omega|E|^2 + \pi\mu''\omega|H|^2 + \sigma|E|^2/2, \quad (1)$$

where E and H respectively denote the electric and magnetic fields of the microwaves, and the double ε and μ respectively indicate imaginary parts of permittivity and magnetic permeability. Additionally, ω is the angular frequency. The three terms on the right-hand side of the equation respectively correspond to the dielectric, magnetic, and conduction loss mechanisms. In the present case, heating was performed in the microwave H-field. Consequently, the first term is not considered important. Although the third term of Eq. (1) is written in terms of the electric field, the conduction current is raised mainly by the induction attributable to the alternating magnetic field H. The tendency of better heating characteristics of conductive materials in the microwave H-field has been described and discussed in an earlier report.[11] The second and the third term become important through the contribution of the H-field.

Because Fe_3O_4 loses ferri-magnetism above the Curie point (T_c) at 520 °C, the magnetic loss mechanism (second term) does not occur above T_c. The main heating mechanism might be the conduction loss at temperatures higher than T_c. In fact, Fe_3O_4 has high electric conductivity ($\sigma \sim 1 \times 10^4$ S/m at RT) because of the hopping conduction of the electron between Fe^{2+} and Fe^{3+}. The conductivity of FeO increases concomitantly with the temperature, although that of Fe_3O_4 does not change considerably with temperature.[14,15] Conductivity of FeO (FeO_{1+x}: wustite, coexisting with magnetite in two phase region in Fig. 7 [13]) increases as an increase of x along the phase boundary (the boundary indicated by an arrow in Fig. 7). As presented in Fig. 8, the conductivity of FeO becomes even higher than that of Fe_3O_4 at 1350 °C (the resistivity is lower[14–16]). The equilibrium composition of FeO shifts to a higher O fraction and FeO_{1+x} becomes more conductive at higher temperatures along

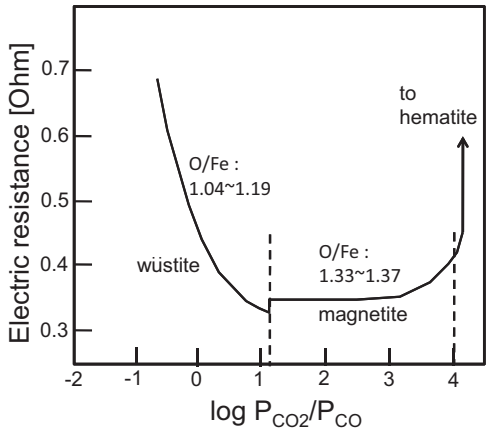

Fig. 8. Electric resistance of Fe_3O_4 and FeO,[14] the data plotted on the phase composition by controlling the CO/CO_2 ratio.[16]

the boundary. Therefore, it is inferred that FeO formation might become more favorable for microwave heating, especially at temperatures higher than 1000 °C, and might cause formation of hot spot regions with a larger fraction of FeO.

4.2. Phase constitution in the hot spot region

The EDX analysis indicating Fe/O compositional difference between the hot spot region and the matrix was not significant (Fig. 3). However, micro-XRD profiles indicated the larger peak height of FeO in the hot spot region. To interpret this fact, it is considered that the phase separation occurred in nanoscale and then caused co-existence of nanoscale FeO, Fe_3O_4, and Fe_2O_3 phases in the hot spot region, as confirmed by TEM observation. Therefore, it is inferred that the spatial fluctuation of oxygen concentration was not resolved by EDX within the probe diameter and that the average oxygen contents are detected. This situation was described in our previous report[10]. The metallic color of the hot spot region might be related with the larger content of FeO and the flat surface.

Morphologies resembling the reported de-crystallization[9] were observed, as portrayed in Fig. 2(b). Their nature remains unclarified, but the features of nano-sized grains and coexistence of multiple phases are consistent with another report.[17]

In our previous report,[10] the mass balance of oxygen in these microstructures was interpreted as follows. The oxygen deficiency in formation of FeO phase was compensated by formation of Fe_3O_4 with larger oxygen content (Fe_3O_4 has considerable oxygen solubility at higher temperature, as presented in Fig. 7, shown with a circle. However, in this study, the microdiffraction peaks of Fe_3O_4 phase from the hot spot region showed little difference from the stoichiometric composition (the lattice parameter of Fe_3O_4). The Fe_2O_3 peaks are apparent (Fig. 6) in the micro-XRD profile. For this reason, occurrence of oxidation during heating with residual oxygen is suspected. If it occurs, then FeO must also be oxidized and not observed in such a great amount. It is known that Fe_2O_3 formation sometimes occurs during high-temperature heating in an inert gas atmosphere.[18] A distinct possibility is that the excess oxygen caused formation of Fe_2O_3, as speculated below. If oxygen transport from FeO to Fe_3O_4 occurred as discussed in an earlier report,[10] then the transport occurred extensively in these hot spot regions, and supplied oxygen in large amounts, engendering the formation of Fe_2O_3. Additional study must be undertaken to clarify the relation of the phase constitution with oxygen composition.

5. Conclusion

Microstructures of hot spot regions formed in the internal regions of the microwave-heated Fe_3O_4 powder were observed using OM, SEM/EDX, normal XRD, micro-XRD, and TEM. Results of EDX analysis indicated that the composition or Fe/O fraction was mostly uniform between the hot spot region and the matrix. However, nanoscale phase separation occurred. Furthermore, according to the micro-XRD peak heights, the fraction of FeO phase was considerably larger in the hot spot region than in the matrix, although the major phase was Fe_3O_4 with only a little Fe_2O_3 phase observed.

Acknowledgements

The authors are grateful for the financial support by Grant-in-Aid of Ministry of Education, Sports, Culture, Science and Technology, Japan, Priority Area on Science and Technology of Microwave-Induced, thermally Non-Equilibrium Reaction Field, and by Grant-in-Aid, Exporatory Research by JSPS.

References

1. Clark DE, Sutton WH. Microwave processing of materials. *Annu Rev Mater Sci* 1996;**26**:299–331.
2. Katz JD. Microwave sintering of ceramics. *Annu Rev Mater Sci* 1992;**22**:153–70.
3. Binner J, Annapoorani K, Paul A, Santacruz I, Vaidhyanathan B. Dense nanostructured zirconia by two stage conventional/hybrid microwave sintering. *J Eur Ceram Soc* 2008;**28**:973–7.
4. Nat. Res. Council, editor. *Microwave processing of materials*. Washington, DC: National Academy Press; 1994. p. 33.
5. Katayose S, Miyazaki T, Hayashi Y, Takizawa H. Synthesis of natural superlattice structure in the binary ZnO–Fe_2O_3 system by microwave irradiation. *J Ceram Soc Jpn* 2010;**118**(5):387–9.
6. Saji T, Izumi M, Morimoto J, Makino Y, Miyake S. *Abstr Autumn Meet Jpn Soc Powder Powder Metall* 2006:69.
7. Peelamedu R, Roy R, Hurtt L, Agrawal D, Fliflet AW, Lewis III D, et al. Phase formation and decrystallization effects on $BaCO_3 + 4Fe_3O_4$ mixtures; a comparison of 83 GHz, multimode millimeter-wave and 2.45 GHz single mode microwave *H*-field processing. *Mater Chem Phys* 2004;**88**:119–29.
8. Roy R, Peelamedu R, Hurtt L, Cheng J, Agrawal D. Definitive experimental evidence for microwave effects: radically new effects of separated E and H fields, such as decrystallization of oxides in seconds. *Mater Res Innovations* 2002;**6**:128–40.
9. Roy R, Peelamedu R, Grimes C, Vheng J, Agrawal D. Major phase transformation and magnetic property changes caused by electromagnetic fields at microwave frequency. *J Mater Res* 2002;**17**(12):3008–11.
10. Yoshikawa N, Cao Z, Louzguin D, Xie G, Taniguchi S. Micro/nanostructure observation of microwave heated Fe_3O_4. *J Mater Res* 2009;**24**(5):1741–7.

11. Yoshikawa N, Ishizuka E, Taniguchi S. Heating of metal particles in a single-mode microwave applicator. *Mater Trans* 2006;**47**(3):898–902.
12. Thostenson ET, Chou TW. Microwave processing: fundamentals and applications. *Compos A* 1999;**30**:1055–71.
13. Kubaschewski O. *Iron-binary phase diagrams*. Berlin, Germany: Springer-Verlag; 1982. pp. 80.
14. Tannhauser DS. Conductivity in iron oxides. *J Phys Chem Solid* 1962;**23**:25–34.
15. Geiger GH, Levin RL, Wagner Ir. JB. Studies on the defect structure of wustite using electrical conductivity and thermoelectric measurements. *J Phys Chem Solid* 1966;**27**:947–56.
16. Darken LS, Gurry RW. *J Am Chem Soc* 1945;**67**:1398–412.
17. Takayama S, Kakurai K, Takeda M, Matsubara A, Nishihara Y, Nishijo J, et al. Investigation of crystal structure formation under microwave heating. *Nucl Instrum Methods Phys Res Sect A* 2009;**600**(1):246–9.
18. M. Sato, Private communication.